

Concurrent higher-order field monitoring for routine head MRI: an integrated heteronuclear setup

C. Barmet¹, B. J. Wilm¹, M. Pavan¹, G. Katsikatsos¹, J. Keupp², G. Mens³, and K. P. Pruessmann¹

¹Institute for Biomedical Engineering, ETH and University, Zurich, Zurich, Switzerland, ²Philips Research Europe, Hamburg, Germany, ³Philips Healthcare, Best, Netherlands

Introduction: Artifacts in MRI are often caused by erroneous dynamic magnetic field behavior. Magnetic field monitoring was recently introduced to observe the actual net magnetic field evolution during MRI scans, irrespective of its sources, which may include gradient coils and amplifiers, eddy currents, magnet drifts, shim dynamics, field changes induced by shim irons, patient breathing, and site-related issues (nearby elevators, trains, etc.) [1]. Once the field evolution is known it can be taken into account at the reconstruction stage, permitting inherent correction of many types of image defects. Field dynamics can be measured by separate calibration [2], which however captures only reproducible effects and misses those of magnet heating, external fields, breathing, etc. It is therefore desirable to perform field monitoring strictly concurrently with each individual scan. As recently shown it can also be important to observe dynamic field perturbations of higher than first order in space [3,4], calling for the use of many field probes in parallel. Jointly these requirements render RF interference between the imaging and monitoring experiments a key challenge. It was previously addressed by RF-shielding of ¹H field probes [5], which however does not permit robust decoupling of large probe arrays. A generic alternative is to base the field probes on another nucleus, which naturally offers spectral decoupling analogous to deuterium locks [6,7]. Finally, for routine scanning patient handling and comfort cannot be compromised. Based on these considerations the present work proposes a heteronuclear 16-channel ¹⁹F field camera integrated with a standard 8-channel ¹H head coil array for routine concurrent field monitoring up to 3rd order in space.

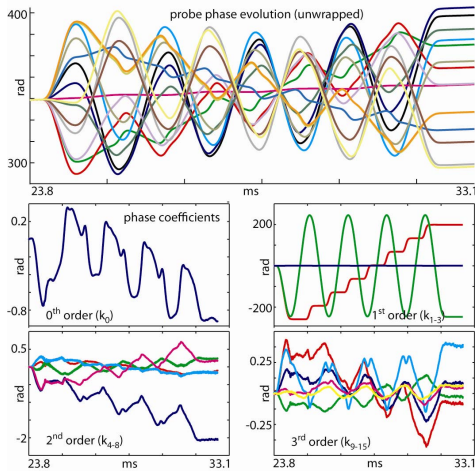


Fig. 4: Top: unwrapped phase evolution of 15 NMR probes over the 9.3 ms readout of the SE-EPI scan. Lower rows: $k_i(t)$ phase coefficient evolution (divided in spatial orders 0-3), as fitted from the probes' phase evolutions and used for image reconstruction. The k_i 's are plotted in 'max notation', i.e. the maximum phase value taken on by $k_i f_i$ inside a sphere with radius 10cm [Eq.1].

maximum phase error inside the sphere (ROI) [Eq.4]. The probe positions were determined by numerically minimizing the cost-function [Eq.5] using the heuristic weights $\alpha_{0-15} = [3,6,6,6,2,2,2,2,1,1,1,1,1,1,1,1]$, which emphasize first order. To match the coil geometry, the probe positions were restricted to a half-sphere of 22.6cm diameter, complemented by a cylinder of 22.6cm diameter and 11.3cm length. Numerically (Monte Carlo) minimizing the cost function ($\rightarrow 0.55$) it was found that an arrangement of three rings with 4, 6 and 5 probes each and one probe at the top of the coil are optimal. Compared to 16 equi-distributed probes on a sphere of 22.6cm diameter ($\rightarrow 0.51$), conditioning is only slightly degraded.

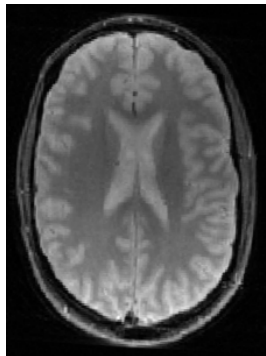


Fig. 5: SE EPI with 24 interleaves, readout dur. 11.20ms, TE 28.7ms, in-plane resolution 1.2mm, slice thickness 4mm. Higher-order image reconstruction [3] is based on k_{0-15} and performed on a cluster of 32 CPU's; reconstruction-time 60sec for 8 coils.

Image reconstruction is exclusively based on the monitored phase coefficients $k_i(t)$. Higher-order image reconstruction accounts for the full phase evolution [Eq.1] and is implemented by an iterative inversion of the complete encoding matrix [4].

To demonstrate the versatility of the integrated setup, head imaging with concurrent 3rd-order monitoring was performed. The SE-EPI scan with 24 interleaves includes strong crusher gradients as well large-angle RF pulses. It highlights the benefits of the heteronuclear setup with independent probe excitation timing that was set right before the acquisition start.

Results and Discussion: The placement of the volunteers' head in the coil array was not affected by the added field-probes. Importantly, the probes' signal lifetimes were not noticeably impaired by static shim effects due to the presence of a head. Field information collected during the 1st interleave of the SE-EPI is shown in Fig. 4. Starting from it, a higher-order image reconstruction yielded the flawless multishot EPI (Fig. 5). Scan protocols do not require any modification for concurrent monitoring, which greatly facilitates its adoption in clinical imaging. Particularly promising applications include scans with long readouts (EPI, spiral), gradient-intensive scans (fMRI, DWI, PC), techniques that are susceptible to eddy currents (spectroscopy, quantitative PC) or field drifts (temperature mapping), as well as all techniques that involve the fusion of data obtained with different sequences (parallel imaging, off-resonance correction). Ultimately, concurrent field monitoring might facilitate the adoption of less costly magnet and gradient hardware.

References: [1] Barmet et al., MRM 60:187 (2008). [2] Duyn et al. JMR 132:150 (1998). [3] Barmet et al., Proc. ISMRM 2009, p.780. [4] Wilm et al., Proc. ISMRM 2009, p.562. [5] Barmet et al., MRM 62:269 (2009). [6] Hofer et al., US patent 4'110'681, 1978. [7] Wiesinger et al., Proc. ESMRMB 2009, p. 109. [8] De Zanche et al., MRM 60:176 (2008).



Fig.2: 8-channel head array with integrated 3rd-order monitoring system. On the right are the four T/R switch- and preamplifier-boards (cf. Fig. 3).

The present work proposes a heteronuclear 16-channel ¹⁹F field camera integrated with a standard 8-channel ¹H head coil array for routine concurrent field monitoring up to 3rd order in space.

Methods: For the integrated monitoring system (Fig.2), 16 NMR probes were mounted on an eight channel head array. The probes are filled with hexafluorobenzene (C₆F₆), doped with 5.5mM Gd(FOD), a complex which dissolves well in non-polar substances and efficiently shortens T₁ without excessively reducing T₂. The probe lifetime was ~ 130 ms, T₁ ~ 190 ms, T₂ ~ 95 ms, inner diameter 1.0 mm, maximum resolution $k_{\max} = (500 \mu\text{m})^{-1}$, SNR $\sqrt{\text{BW}} = 5.4 \cdot 10^4 \sqrt{\text{Hz}}$ [8]. The ¹⁹F probes are operated in transmit/receive (T/R) mode and simultaneously excited by hard RF pulses in the microsecond range, generated by a separate transmit chain [5]. The probe excitation trigger is introduced as a sequence object, it is freely programmable and typically set at the ¹H excitation time or just before the acquisition start; this flexibility is a consequence of the spectral separation of ¹⁹F and ¹H. The resulting probe NMR signals are received via custom-built T/R switches with integrated preamplifiers (Fig.3) and fed into 16 channels of the system spectrometer (3T Philips Achieva, Philips Healthcare, Best, NL). Four spectrometer boards (4 channels each) were programmed to receive the ~ 120.2 MHz probe signal while two other boards selected the band around 127.8 MHz (¹H coil-data); ¹⁹F and ¹H signals were concurrently acquired and the sampling rate was identical for all 24 channels.

To extract the phase coefficients k_0-k_{15} [1], the phase of the probe signals is unwrapped and fitted to a spatial model [Eq.1], using the 16 basis fcts. $f_\lambda(r) [\lambda: 0 \rightarrow 15]$ that constitute a full 3rd order, real-valued spherical harmonic expansion [3,4] (Fig.4). Care must be taken when choosing the probe positions, for they determine the conditioning of the model fit [Eq.1] [1]. Starting from the phase error of the probe's phase data [Eq.2], the error on the phase coefficient k_i is given by Eq.3 (+ denotes the pseudo-inverse). For each λ , this leads to a

$$\phi(r,t) = \sum_{\lambda} k_{\lambda}(t) \cdot f_{\lambda}(r) \quad [1]$$

$$\sigma_p = 1/(\sqrt{2} \text{SNR}) \quad [2]$$

$$\sigma_{k,\lambda} = \sigma_p \sum_j (P_{\lambda,j}^+)^2 \quad [3]$$

$$\sigma_{\phi,\lambda,\max} = \sigma_{k,\lambda} \cdot \max_{ROI} [f_{\lambda}(r)] \quad [4]$$

$$\sum_{\lambda} \alpha_{\lambda} \cdot \sigma_{\phi,\lambda,\max} \quad [5], [4]$$

Fig. 1: Equations 1-5.

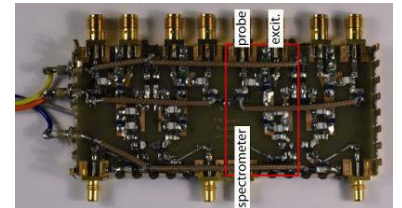


Fig.3: 4 T/R switches and preamplifiers (operating 4 probes) were integrated on one board and RF-shielded by a box. It is connected to a driver board that delivers the power for the preamplifiers, voltage for T/R switching and assures coil identification. Four of these boxes have been used to operate 16 probes.